

Indirect band gap of coherently strained $\text{Ge}_x\text{Si}_{1-x}$ bulk alloys on $\langle 001 \rangle$ silicon substrates

R. People

AT&T Bell Laboratories, Murray Hill, New Jersey 07974

(Received 11 April 1985)

Estimates of the indirect band gap for coherently strained alloys of $\text{Ge}_x\text{Si}_{1-x}$ on Si(001) are given for x in the range $0 \leq x \leq 0.75$. The present results were obtained by combining x-ray diffraction data with relevant deformation-potential constants and using the phenomenological strain Hamiltonian of Kleiner and Roth. Uniaxial splittings of the sixfold-degenerate valence-band edge were calculated using the 6×6 Hamiltonian of Hasegawa. It is found that the coherency strain generated by lattice mismatch dramatically reduces the indirect gap of the alloy (which approaches the $L_1-\Gamma_{25}'$ gap of unstrained Ge at $x \approx 0.6$).

I. INTRODUCTION

A quantitative determination of the growth parameters pertinent to the pseudomorphic growth of $\text{Ge}_x\text{Si}_{1-x}$ /Si strained layers¹ has resulted in the recent observation of the modulation-doping effect,² the integration of a Ge *p-i-n* photodetector on a Si substrate,³ and the fabrication of a modulation doped $\text{Ge}_x\text{Si}_{1-x}$ /Si field-effect transistor.⁴ The applicability of the present system for fabrication of other novel optoelectronic devices (e.g., "quasi-direct-gap" photodetectors and staircase-avalanche photodetectors⁵) rests heavily upon a knowledge of the indirect band gap of the coherently strained alloy and the relative alignment of the alloy-Si band edges. The present study addresses the former issue.

Resonant Raman scattering⁶ has demonstrated that heteroepitaxy of commensurate $\text{Ge}_x\text{Si}_{1-x}$ on Si results in strained layers for which the entire lattice mismatch is accommodated as a homogeneous tetragonal strain in the alloy layers only. This fact allows for the calculation of the in-plane lattice distortions solely in terms of the bulk-alloy lattice parameters.⁷ Further, Rutherford backscattering⁸ techniques have demonstrated that the magnitude of the tetragonal distortion (e_T) in the alloy is described well by elasticity theory, which allows one to determine e_T in terms of the lattice mismatch f . It is therefore straightforward to determine the compositional dependence of the components of the strain tensor.

These alloy-dependent components of the strain tensor along with the relevant deformation potentials allow a complete description of the motion-of-alloy band edges in terms of the strain Hamiltonian as first introduced by Kleiner and Roth.⁹ The shifts of the indirect-conduction-band edges are described within the formalism of Herring and Vogt.¹⁰ The indirect band gap of the strained alloy will therefore consist of four contributions: (i) band gap of the unstrained alloy,¹¹ (ii) uniform shifts of the band gap due to dilation (i.e., hydrostatic terms), (iii) uniaxial splittings of the indirect- (Δ_1) conduction-band edges, and (iv) uniaxial splittings of the degenerate valence edge at $\mathbf{k}=0$. The compositional dependence of the strain tensor will first be considered.

II. STRAIN TENSOR FOR THE ALLOY

Commensurate growth of $\text{Ge}_x\text{Si}_{1-x}$ strained layers on Si(001) results in a biaxial in-plane compression of the al-

loy and an extension normal to the plane of the $\text{Ge}_x\text{Si}_{1-x}$ /Si interface. This tetragonal distortion of the alloy results in a very simple form for the strain tensor e_{ij} . If one defines $\mathbf{z} \parallel [001]$ (i.e., along the growth direction) then e_{ij} has only diagonal components. The assumption of a rigid Si lattice leads to

$$e_{xx} = e_{yy} = \left(\frac{a_0 - b(x)}{b(x)} \right) < 0, \quad (1a)$$

where a_0 and $b(x)$ are the Si and alloy lattice constants,⁷ respectively. The extension e_{zz} of the alloy along the growth direction is obtained from the expression

$$e_{zz} - e_{xx} = \left(\frac{1 + \nu}{1 - \nu} \right) f, \quad (1b)$$

where the lattice mismatch f is defined as

$$f \equiv \left(\frac{b(x) - a_0}{a_0} \right), \quad (1c)$$

and Poisson's ratio ν varies between 0.273 for Ge and 0.280 for Si. Equations (1a)–(1c) define the compositional dependence of the alloy strain tensor.

III. UNIAXIAL SPLITTINGS OF THE VALENCE-BAND EDGE

The valence-band edge of Ge and Si is threefold degenerate in the absence of spin and transforms as Γ_{25}' of the cubic group O_h .¹² The inclusion of spin produces six states which are split by the spin-orbit interaction into a fourfold ($J = \frac{3}{2}$) state having symmetry Γ_8^+ and a twofold ($J = \frac{1}{2}$) set of states having Γ_7^+ symmetry. At present we are interested in the splittings of these states (at $\mathbf{k}=0$) produced by lattice-mismatch-induced coherency strains. As previously stated, alloys grown on Si(001) substrates experience a tetragonal distortion, wherein the nonzero elements of the strain tensor satisfy $e_{xx} = e_{yy} < 0$, $e_{zz} > 0$, $e_{ij} = 0$, $i \neq j$. For small values of the strain, the strain Hamiltonian can be written in (4×4) matrix form with basis operators of the angular momentum \mathbf{J} ($J = \frac{3}{2}$) to represent the interactions "within" the $J = \frac{3}{2}$ multiplet; the resulting expressions for a strain Hamiltonian are given by Hensel and Feher.¹³ The 4×4 Hamiltonians, though convenient, do not suffice for

the present purpose since the large strains encountered in the $\text{Ge}_x\text{Si}_{1-x}/\text{Si}$ system induce non-negligible off-diagonal terms which couple the $J = \frac{3}{2}$ and $\frac{1}{2}$ bands. The 6×6 strain Hamiltonian required for an accurate description of the valence-band splittings under high stress has been given by Hasegawa.¹⁴ It should be noted that for [001] distortions the strain operators couple only those states of $J = \frac{3}{2}$ and $\frac{1}{2}$ which have the same magnetic quantum number $\pm M_J$ (i.e., $\pm M_J$ remains a good quantum number). This means that the eigenstates at $\mathbf{k} = 0$ can be uniquely represented by (J, M_J) descriptors. The resulting strain Hamiltonian can be readily diagonalized and yields three eigenvalues at $\mathbf{k} = 0$ (each doubly degenerate) whose alloy dependences are given by

$$E_v(\frac{3}{2}; \pm \frac{3}{2}) = \epsilon(x) , \quad (2a)$$

$$E_v(\frac{3}{2}; \pm \frac{1}{2}) = -\frac{1}{2}[\epsilon(x) + \Lambda] + \frac{1}{2}\sqrt{9\epsilon^2(x) + \Lambda^2 - 2\epsilon(x)\Lambda} , \quad (2b)$$

and

$$E_v(\frac{1}{2}; \pm \frac{1}{2}) = -\frac{1}{2}[\epsilon(x) + \Lambda] - \frac{1}{2}\sqrt{9\epsilon^2(x) + \Lambda^2 - 2\epsilon(x)\Lambda} . \quad (2c)$$

The strain energy $\epsilon(x)$ is a function of alloy composition and is given by

$$\epsilon(x) = \frac{2}{3}D_u(x)e_T(x) = \frac{2}{3}D_u(x)[e_{zz}(x) - e_{xx}(x)] , \quad (3)$$

where D_u is the valence-band deformation potential associated with [001] distortions, Λ denotes the spin-orbit splitting, and x denotes the Ge content of the alloy. We have used the following values for the deformation potential D_u :

$$D_u = \begin{cases} (2.04 \pm 0.2) \text{ eV for Si (Ref. 13),} \\ (3.81 \pm 0.25) \text{ eV for Ge (Ref. 15),} \end{cases} \quad (4)$$

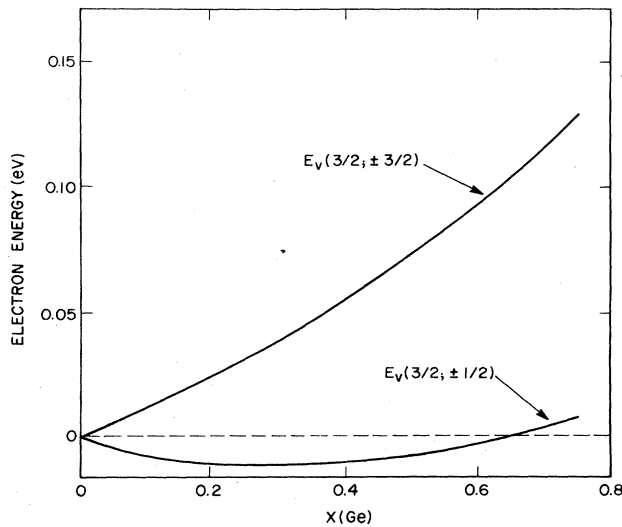


FIG. 1. Uniaxial splittings of the upper ($J = \frac{3}{2}$) valence-band edge of bulk $\text{Ge}_x\text{Si}_{1-x}$ alloys on Si(001) substrates. The states are labeled by (J, M_J) representation.

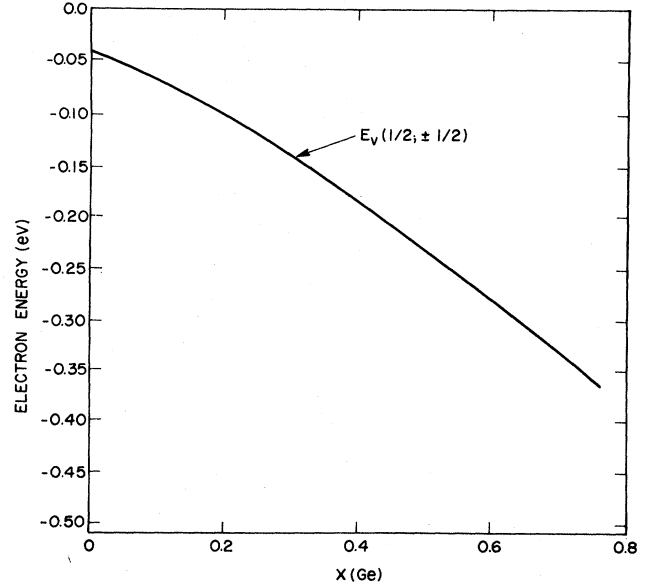


FIG. 2. Uniaxial splitting of spin-orbit split off ($J = \frac{1}{2}$) valence-band edge for bulk $\text{Ge}_x\text{Si}_{1-x}$ alloys grown on Si(001) substrates.

and a linear interpolation for the alloy dependence of D_u . In like manner we allow the spin-orbit splitting $\Lambda(x)$ to vary linearly between 0.044 eV for Si to 0.29 eV for Ge. These results have been plotted in Figs. 1 and 2. Note that the lowest-lying valence-band edge is the doublet $E_v(\frac{3}{2}; \pm \frac{3}{2})$, which moves up in electron energy as x increases.

IV. UNIAXIAL SPLITTINGS OF THE Δ_1 CONDUCTION-BAND EDGES

Since we restrict x to the range $0 \leq x \leq 0.75$, the alloy conduction band is Si-like,¹¹ i.e., minimum at Δ_1 , along [001] directions. For conduction-band minima off the center of the Brillouin zone, the shapes of the constant-energy surfaces are unchanged to first order in strain, whereas the extremum energy of a particular valley will depend on both the magnitude of the strains and their directions with respect to the \mathbf{k} vector of the valley of interest.

Herring and Vogt¹⁰ have shown that the energy shift $\Delta E_c^{(i)}$ of valley " i ," for an arbitrary deformation can be described by

$$\Delta E_c^{(i)} = [\Xi_d \bar{\mathbf{I}} + \Xi_u (\hat{\mathbf{a}}_i \hat{\mathbf{a}}_i)] : \bar{\boldsymbol{\epsilon}} \quad (5)$$

in terms of the deformation potentials Ξ_d and Ξ_u (d denotes dilation and u implies uniaxial). Here $\bar{\mathbf{I}}$ is the unit tensor, $\hat{\mathbf{a}}_i$ is a unit vector parallel to the \mathbf{k} vector of valley i , and $\hat{\mathbf{a}}_i \hat{\mathbf{a}}_i$ denotes a dyadic product. The shift of the mean energy of the band extrema was found to equal

$$\Delta E_c^{(0)} = (\Xi_d + \frac{1}{3}\Xi_u) \bar{\mathbf{I}} : \bar{\boldsymbol{\epsilon}} . \quad (6)$$

The uniaxial splitting of the i th valley is then given by the

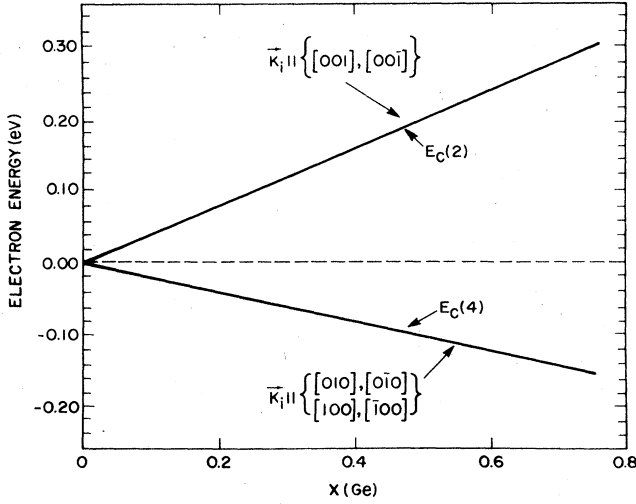


FIG. 3. Δ_1 conduction-band splitting (uniaxial components only) for bulk $\text{Ge}_x\text{Si}_{1-x}$ alloys grown on Si(001) substrates.

difference in Eqs. (5) and (6), namely,

$$\Delta E_c^{(i)} - \Delta E_c^{(0)} = \begin{cases} \frac{2}{3}\Xi_u e_T \text{ for } \mathbf{k}^{(i)} \parallel \{[001], [00\bar{1}]\}, \\ -\frac{1}{3}\Xi_u e_T \text{ for } \mathbf{k}^{(i)} \parallel \left\{ \begin{matrix} [010], [0\bar{1}0] \\ [100], [100] \end{matrix} \right\}. \end{cases} \quad (7)$$

It will be noted that since both $\Xi_u, e_T(x) > 0$ the lowest conduction-band minima is fourfold degenerate in the strained bulk alloy. We have used $\Xi_u = \Xi_u^{[001]}(\text{Si}) = 9.2 \text{ eV}$.¹⁶ No alloy dependence of Ξ_u has been assumed. The alloy dependence of the band-edge shifts in Eq. (7) are plotted in Fig. 3.

V. HYDROSTATIC CONTRIBUTION TO THE ALLOY BAND GAP

Equations (2) and (7) give the uniaxial splittings of the valence- and conduction-band edges as a function of alloy composition. In order to compute the various band gaps (i.e., conduction- to valence-band energy separations) one also needs to determine the change in alloy band gap due to dilations (i.e., $\Delta V/V \neq 0$, $V \equiv$ volume of the crystal). These contributions will be referred to as hydrostatic terms. From Eq. (6) it is readily seen that the deformation potential appropriate for describing the hydrostatic term is $(\Xi_d + \frac{1}{3}\Xi_u - a)$, where a denotes the deformation potential which describes uniform shifts of the valence-band edge.¹⁷ Hence,

$$\Delta E_{\text{hydro}} = (\Xi_d + \frac{1}{3}\Xi_u - a)\bar{\epsilon}. \quad (8)$$

We have used

$$(\Xi_d + \frac{1}{3}\Xi_u - a) = \begin{cases} +3.8 \text{ eV for Si (Ref. 18)}, \\ -2.9 \text{ eV for Ge (Ref. 18)}. \end{cases} \quad (9)$$

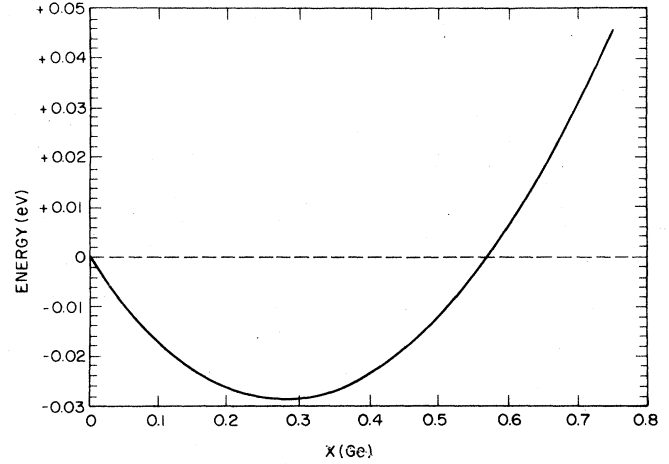


FIG. 4. Hydrostatic contribution to the indirect band gap of coherently strained bulk $\text{Ge}_x\text{Si}_{1-x}$ alloys, for growth on Si(001) substrates.

Note that the sign of $(\Xi_d + \frac{1}{3}\Xi_u - a)$ is opposite and negative for Ge. Since $\Delta V/V < 0$, for $\text{Ge}_x\text{Si}_{1-x}$ alloys on Si(001), it is seen that when these alloys have Si-like band structures the hydrostatic terms are expected to produce a uniform decrease of the indirect band edge, whereas this trend is reversed for Ge-like band edges. $(\Delta V/V)$ decreases monotonically with increasing Ge content and is approximately -3.7% at $x=0.75$. Equation (8) is plotted in Fig. 4, where we have assumed a linear interpolation for $(\Xi_d + \frac{1}{3}\Xi_u - a)$ between the values for Si and Ge. This assumption is expected to give an upper bound on the alloy band gap in that $(\Xi_d + \frac{1}{3}\Xi_u - a)$ is likely to remain Si-like and to vary with composition in a manner similar to the fundamental band gap of the unstrained alloy,⁹ showing an abrupt change in sign and magnitude for $x \geq 0.85$. Clearly, an experimental determination of the compositional dependence of the band gap of these strained alloys will be necessary in order to properly evaluate these deformation potentials.

VI. RESULTS AND DISCUSSION

The results of Eqs. (2), (7), and (8) have been combined with the unstrained bulk-alloy band-gap data of Braunstein, Moore, and Herman¹¹ to yield the indirect gap for coherently strained $\text{Ge}_x\text{Si}_{1-x}$ alloys grown on Si(001) substrates. These data are plotted in Fig. 5. It will be noted that coherency strain dramatically reduces the alloy band gap to such an extent that for $x \approx 0.6$ the strained-alloy band gap becomes equal to the indirect band gap of unstrained Ge ($E_g \sim 0.66 \text{ eV}$). The width of the strained-alloy band gap reflects an uncertainty in our knowledge of the various deformation potentials involved; note, however, that this uncertainty does not exceed $\sim 75 \text{ meV}$ for $x < 0.75$.

Low-temperature ($T \leq 10 \text{ K}$) sheet charge-density measurements have been used to estimate the band gap of the strained alloy for $x=0.2$. Assuming the majority of the band offset to be in the valence band,² it is estimated that $0.88 \text{ eV} \leq E_{\text{gap}} \leq 0.92 \text{ eV}$, in good agreement with the

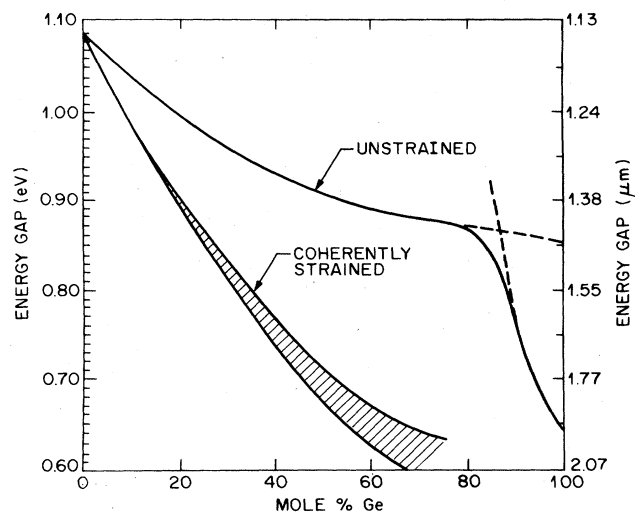


FIG. 5. Indirect band gap of coherently strained bulk $\text{Ge}_x\text{Si}_{1-x}$ alloys for growth on Si(001) substrates.

present results. These results are extremely exciting insofar as potential applications of these strained-alloy layers to long-wavelength optical devices are concerned. They imply that more dilute alloys may be used to access the $1.55\text{-}\mu\text{m}$ wavelength range, thereby reducing the tendency of islanding during growth and improving the stability of these alloys at temperatures required for device processing. Further, the large band-edge offsets deduced from the present results, coupled with the suspected gross asymmetry of the band-edge offsets predicted by transport measurements,² make these alloys potential candidates for such novel photodetectors as the staircase and superlattice photodiodes discussed by Capasso.⁵

ACKNOWLEDGMENTS

I would like to thank A. Y. Cho and V. Narayanamurti for continued encouragement in the course of the present work. I have also benefited greatly from discussions with J. C. Bean, A. C. Gossard, and J. C. Hensel.

- ¹J. C. Bean, L. C. Feldman, A. T. Fiory, S. Nakahara, and I. K. Robinson, *J. Vac. Sci. Technol. A* **2**, 436 (1984).
- ²R. People, J. C. Bean, D. V. Lang, A. M. Sargent, H. L. Störmer, K. W. Wecht, R. T. Lynch, and K. Baldwin, *Appl. Phys. Lett.* **45**, 1231 (1984).
- ³S. Luryi, A. Kastalsky, and J. C. Bean, *IEEE Trans. Electron Devices* **ED-31**, 1135 (1984).
- ⁴T. P. Pearsall, J. C. Bean, and R. People *Appl. Phys. Lett.* (to be published).
- ⁵F. Capasso, *Surf. Sci.* **132**, 527 (1983).
- ⁶F. Cerdeira, A. Pinczuk, J. C. Bean, B. Batlogg, and B. A. Wilson, *Appl. Phys. Lett.* **45**, 1138 (1984).
- ⁷J. P. Dismukes, L. Ekstrom, and R. J. Paff, *J. Phys. Chem.* **68**, 3021 (1964).
- ⁸J. C. Bean, T. T. Sheng, L. C. Feldman, A. T. Fiory, and R. T. Lynch, *Appl. Phys. Lett.* **44**, 102 (1984).
- ⁹W. H. Kleiner and L. M. Roth, *Phys. Rev. Lett.* **2**, 334 (1959).
- ¹⁰C. Herring and E. Vogt, *Phys. Rev.* **101**, 944 (1956).
- ¹¹R. Braunstein, A. R. Moore, and F. Herman, *Phys. Rev.* **109**, 695 (1958).
- ¹²G. F. Koster, in *Solid State Physics*, edited by F. Seitz and D. Turnbull (Academic, New York, 1957), Vol. 5, p. 173.
- ¹³J. C. Hensel and G. Feher, *Phys. Rev.* **129**, 1041 (1963).
- ¹⁴H. Hasegawa, *Phys. Rev.* **129**, 1029 (1963).
- ¹⁵J. C. Hensel and K. Suzuki, *Phys. Rev. B* **9**, 4219 (1974).
- ¹⁶I. Balslev, *Phys. Rev.* **143**, 636 (1965).
- ¹⁷G. E. Pikus and G. L. Bir, *Fiz. Tverd. Tela.* **1**, 1642 (1959) [*Sov. Phys. Solid State* **1**, 1502 (1960)].
- ¹⁸G. L. Bir and G. E. Pikus, *Symmetry and Strain-Induced Effects in Semiconductors* (Wiley, New York, 1974), p. 469.